



# Technical note: Photosynthetic capacity estimation is dependent on model assumptions

Yujie Wang<sup>1</sup> and Christian Frankenberg<sup>1,2</sup>

<sup>1</sup>Division of Geological and Planetary Sciences, California Institute of Technology, Pasadena, California 91125, USA

<sup>2</sup>Jet Propulsion Laboratory, California Institute of Technology, Pasadena, California 91109, USA

**Correspondence:** Yujie Wang (wyujie@caltech.edu)

**Abstract.** Modeling leaf photosynthesis is crucial for Earth system modeling. However, as photosystem light absorption and gas exchange are not typically simultaneously measured, photosynthetic capacity estimation and thus photosynthesis modeling are subject to inaccurate light absorption representation in photosynthesis models. We analyzed how leaf absorption features and light source may impact photosynthesis modeling at various settings. We found that (1) estimated photosynthetic capacity can be over- or under-estimated depending on model assumption, and the bias increases with higher mismatch in leaf light absorption parameters and higher true capacity; and (2) modeled photosynthetic rate can also be over- or under-estimated depending on model assumption, and the bias increases with higher leaf internal CO<sub>2</sub>, and increases and then decreases with increasing light intensity. We recommend researchers not to mix and match results or models with inconsistent assumptions when modeling photosynthesis.

## 10 1 Introduction

Accurately estimating leaf photosynthetic capacity is crucial to model vegetation carbon, water, and energy fluxes at various scales. Photosynthetic capacity in C3 plants is typically represented by maximum carboxylation rate— $V_{\text{cmax}25}$  at 25 °C, and maximum electron transport rate— $J_{\text{max}25}$  at 25 °C for C3 plants (see Table 1 for the list of symbols).  $V_{\text{cmax}25}$  and  $J_{\text{max}25}$  are typically estimated from  $A \sim C_i$  curves, measurements of net photosynthetic rates ( $A$ ) at different internal CO<sub>2</sub> concentrations ( $C_i$ ) under saturated light. However, as photosynthesis measurements do not include leaf hyperspectral absorption features, researchers often have to assume how much photosynthetically active radiation (PAR) is absorbed by leaf (APAR), and how much of this is absorbed by the antenna system of the photosystems (PPAR), or how much PPAR may contribute to potential electron transport in photosystem II ( $J_{\text{PAR}}$ ; not actual  $J$ ):

$$\text{APAR} = \text{PAR} \cdot f_{\text{APAR}}, \quad (1)$$

$$20 \quad \text{PPAR} = \text{APAR} \cdot f_{\text{PPAR}}, \quad (2)$$

$$J_{\text{PAR}} = \text{PPAR} \cdot f_{\text{PSII}} \cdot \Phi_{\text{PSII,max}}. \quad (3)$$



**Table 1.** List of symbols.

Symbol	Description
$A$	Net photosynthetic rate
$C_i$	Internal CO <sub>2</sub> concentration
$J$	Potential electron transport rate
$J_{PAR}$	Maximum potential electron transport rate
$J_{max}$	Maximum electron transport rate at leaf temperature
$J_{max25}$	Maximum electron transport rate at 25 °C (C3)
$R_d$	Respiration rate
$V_{cmax25}$	Maximum carboxylation rate at 25 °C (C3 and C4)
$V_{pmax25}$	Maximum PEP carboxylation rate at 25 °C (C4)
$\Gamma^*$	CO <sub>2</sub> compensation point with the absence of $R_d$
$\theta$	Smoothing curvature to compute $J$
Car	Carotenoid content
Chl	Chlorophyll content
LMA	leaf dry mass per area
APAR	PAR absorbed by leaf
PAR	Photosynthetically active radiation
PPAR	PAR absorbed by antenna system of the photosystems
$f_{APAR}$	Fraction of APAR in PAR (APAR/PAR)
$f_{PPAR}$	Fraction of PPAR in APAR (PPAR/APAR)
$f_{PSII}$	Fraction of PPAR goes to photosystem II
$\Phi_{PSII,max}$	Maximum photosystem II yield
$\alpha$	Electron quantum yield ( $f_{APAR} \cdot f_{PPAR} \cdot f_{PSII} \cdot \Phi_{PSII,max}$ )

where  $f_{APAR}$  is the fraction of PAR absorbed by leaf,  $f_{PPAR}$  is the fraction of APAR that goes to photosystems,  $f_{PSII}$  is the fraction of PPAR that goes to photosystem II (typically assumed to be 0.5), and  $\Phi_{PSII,max}$  is maximum photosystem II yield (typically assumed to be constant, e.g., 0.82 as in van der Tol et al. (2014) and 0.85 as in Quebbeman and Ramirez (2016)).

25 In theory,  $f_{APAR}$  and  $f_{PPAR}$  are dependent on leaf biophysical parameters (such as leaf dry mass, pigment contents, and water content) and incoming radiation spectrum (Jacquemoud and Baret, 1990; Féret et al., 2017). Fig. 1a shows the absorption coefficients of chlorophyll, carotenoid, water, and leaf dry matter; Fig. 1b shows both  $f_{APAR}$  and  $f_{PPAR}$  using the PROSPECT leaf radiative transfer model (Jacquemoud and Baret, 1990) using the specified leaf pigment composition. For example, if chlorophyll content decreases, both  $f_{APAR}$  and  $f_{PPAR}$  decrease, and hence  $f_{APAR} \cdot f_{PPAR}$ , which is in principle a first-principles calculation of the action spectrum of photosynthesis (Fig. 1c). We note that leaf optical models may have different assumptions on PPAR absorption, e.g. Wang et al. (2021) started to account for both chlorophyll and carotenoid absorption as PPAR as



carotenoid belongs to the antenna system, and ignoring the carotenoid PPAR contribution would result in underestimated  $f_{APAR} \cdot f_{PPAR}$ . Thus, it is important to be aware of model assumptions when using models to compute PPAR.

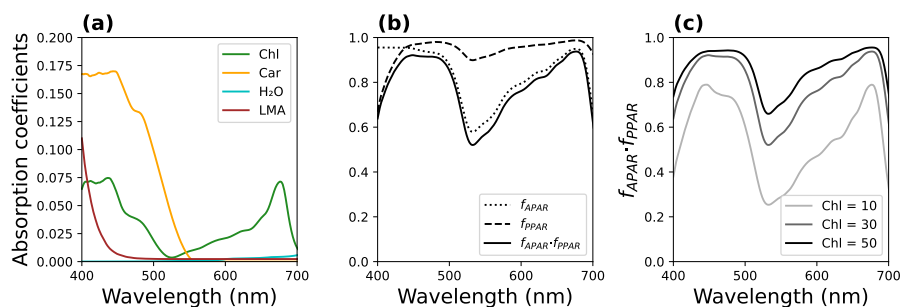


**Figure 1.** Hyperspectral leaf absorption features. (a) Absorption coefficients of Chl (coefficient unit:  $\text{cm}^2 \mu\text{g}^{-1}$ ), Car (coefficient unit:  $\text{cm}^2 \mu\text{g}^{-1}$ ), water (coefficient unit:  $\text{cm}^{-1}$ ), and LMA (coefficient unit:  $\text{cm}^2 \text{mg}^{-1}$ ). (b)  $f_{APAR}$  and  $f_{PPAR}$  spectra. (c)  $f_{APAR} \cdot f_{PPAR}$  at different chlorophyll contents (Chl unit:  $\mu\text{g cm}^{-2}$ ). See Table 1 for the list of symbols. The spectra are simulated using the LeafOptics.jl module of the CliMA Land (Wang et al., 2021).

Further, as leaf absorption in the PAR range is not spectrally uniform, adjusting  $f_{APAR}$  and  $f_{PPAR}$  based on the actual emission spectrum of the light source is therefore necessary to accurately model photosynthesis. Thus, one needs to be cautious regarding the light source when utilizing empirical correlation between chlorophyll content vs.  $f_{APAR}$  and  $f_{PPAR}$  (Evans, 1996; Quebbeman and Ramirez, 2016). For example, a Licor portable photosynthesis system has its blue/red light peaked at 453/660 nm, respectively (corresponding to the peaks of PPAR absorption; Fig. 1). In comparison, natural light in the PAR range has a larger contribution from green light for both direct and diffuse light (wavelength c. 550 nm; Fig. 2a). As a result, Evans (1996) found  $f_{APAR} \cdot f_{PPAR}$  to be  $> 0.9$  for leaves with high chlorophyll content using artificial red and blue light (also see our simulated solid curve for Licor in Fig. 2b). The difference between artificial and natural light may be  $> 0.2$  for  $f_{APAR} \cdot f_{PPAR}$  even when the leaf chlorophyll content (Chl) is measured and used to compute the leaf absorption (Fig. 2b).

The bias in  $f_{APAR} \cdot f_{PPAR}$  could be much higher if chlorophyll and other pigments are not accurately accounted for. Due to the lack of hyperspectral measurements along with leaf gas exchange,  $\alpha = f_{APAR} \cdot f_{PPAR} \cdot f_{PSII} \cdot \Phi_{PSII, \max}$  is often assumed to be constant when estimating photosynthetic capacities from  $A \sim C_i$  curves. For example, Medlyn et al. (2002) and Sperry et al. (2017) used an  $\alpha = 0.3$ , and Harley et al. (1992) and Walker et al. (2014) used an  $\alpha = 0.24$ . While the bias in assuming a fixed  $f_{APAR} \cdot f_{PPAR}$  under artificial blue and red light is small under high chlorophyll conditions ( $> 20 \mu\text{g cm}^{-2}$ ), it increases substantially at lower chlorophyll concentrations (Fig. 2b). Under natural light,  $f_{APAR} \cdot f_{PPAR}$  also shows a higher sensitivity to the chlorophyll content, though differs slightly between direct and diffuse light (Fig. 2b). Our model simulations showed that  $f_{APAR} \cdot f_{PPAR}$  is below 0.75/0.71 even for very high chlorophyll content under natural direct/diffuse light, and this corresponds to a maximum  $\alpha$  of 0.31/0.29, respectively. However, for example, the state-of-art community land model (CLM; version 5) uses a  $f_{APAR} \cdot f_{PPAR}$  ranging from 0.84 to 0.88, corresponding to a constant  $\alpha$  from 0.36 to 0.38 (plant function type based; independent of direct/diffuse light or chlorophyll content) (Lawrence et al., 2019).

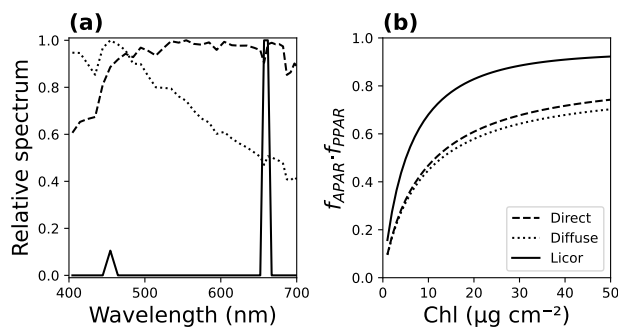


**Figure 2.** Leaf light absorption at different chlorophyll contents for three spectra. **(a)** Three relative spectra used to derive leaf absorption. Dashed/dotted curve plots the natural direct/diffuse light (data from CliMA Land; Wang et al., 2021). Solid curve plots the artificial light mimicking the Licor portable photosynthesis system (5% blue light and 95% red light). **(b)** Leaf absorption at different chlorophyll contents. See Table 1 for the list of symbols. The spectra are simulated using the LeafOptics.jl module of the CliMA Land (Wang et al., 2021).

Thus, inaccurate representation of leaf PAR absorption could potentially result in errors in photosynthesis modeling, such as fitted  $J_{\max25}$  and modeled photosynthetic rate when photosynthesis is limited by RuBP regeneration. Note here that  $V_{\max25}$  is fitted from the RubisCO-limited part of an  $A \sim C_i$  curve, so that  $V_{\max25}$  estimation and RibusCO-limited photosynthetic rate are not supposed to be biased by electron transport modeling.

## 2 Biased maximum electron transport rate

$J_{\max25}$  is fitted from the light-limited part of an  $A \sim C_i$  curve (Farquhar et al., 1980):

$$A = \frac{J}{4} \cdot \frac{C_i - \Gamma^*}{C_i + 2\Gamma^*} - R_d, \quad (4)$$

where  $J$  is the potential electron transport rate,  $\Gamma^*$  is the  $\text{CO}_2$  compensation point with the absence of dark respiration, and  $R_d$  is the respiration rate.  $J$  is typically computed through smoothing  $J_{\text{PAR}}$  and maximum electron transport rate ( $J_{\max}$  at leaf temperature), and the commonly seen smoothing algorithms (Smith, 1937; Wullschleger, 1993; Medlyn et al., 2002) are

$$J = \frac{J_{\text{PAR}} + J_{\max} - \sqrt{(J_{\text{PAR}} + J_{\max})^2 - 4\theta J_{\text{PAR}} J_{\max}}}{2\theta}, \quad (5)$$

$$J = \frac{J_{\text{PAR}} J_{\max}}{\sqrt{J_{\text{PAR}}^2 + J_{\max}^2}}, \quad (6)$$

where  $0 < \theta \leq 1$  is the smoothing curvature (e.g., Medlyn et al. (2002) and Sperry et al. (2017) used 0.9, Lawrence et al. (2019) and von Caemmerer (2021) used 0.7). In the present study, we used equation 5 to smooth  $J$  as  $\theta$  can be tuned. Because of the smoothing algorithm, it is expected that inaccurate  $\alpha$  and  $\theta$  could both result in biased  $J_{\max25}$  estimation.

To evaluate how the estimated  $J_{\max25}$  depends on  $\alpha$  and  $\theta$ , we generated surrogate  $A \sim C_i$  curves by iterating true Chl from 1 to 50  $\mu\text{g cm}^{-2}$  ( $\alpha$  from Fig. 2b for Licor light source), true  $\theta$  from 0.05 to 1, and true  $V_{\max25}$  from 20 to 120  $\mu\text{mol m}^{-2} \text{s}^{-1}$



( $J_{\max25} = 2V_{\max25}$ ). All  $A \sim C_i$  curves were modeled at a given PAR of  $1600 \mu\text{mol m}^{-2} \text{s}^{-1}$  and leaf temperature of  $25 \text{ }^\circ\text{C}$  using the Photosynthesis.jl module of CliMA Land (Wang et al., 2021). Per  $A \sim C_i$  curve, we fitted apparent  $V_{\max25}$  and  $J_{\max25}$  using constant  $\alpha = 0.3$  (equivalent to a Chl of  $13 \mu\text{g cm}^{-2}$ ) and  $\theta = 0.7$  (equation 5).

When we varied true Chl from 1 to  $50 \mu\text{g cm}^{-2}$ , we found that fitted  $J_{\max25} : V_{\max25}$  increased with higher true Chl for all tested  $\theta$  and  $V_{\max25}$  combinations (Fig. 3a). When we varied true  $\theta$  from 0.05 to 1, we found that fitted  $J_{\max25} : V_{\max25}$  increased with higher true  $\theta$  for all tested Chl and  $V_{\max25}$  combinations (Fig. 3b). When we varied true  $V_{\max25}$  ( $J_{\max25} = 2V_{\max25}$ ), we found that fitted  $J_{\max25} : V_{\max25}$  decreased with higher true  $V_{\max25}$  when fitted  $J_{\max25}$  was underestimated, but increased with higher true  $V_{\max25}$  when fitted  $J_{\max25}$  was overestimated (Fig. 3c). Our results highlight the importance of accounting for leaf absorption features and smoothing curvature in estimating  $J_{\max25}$ .

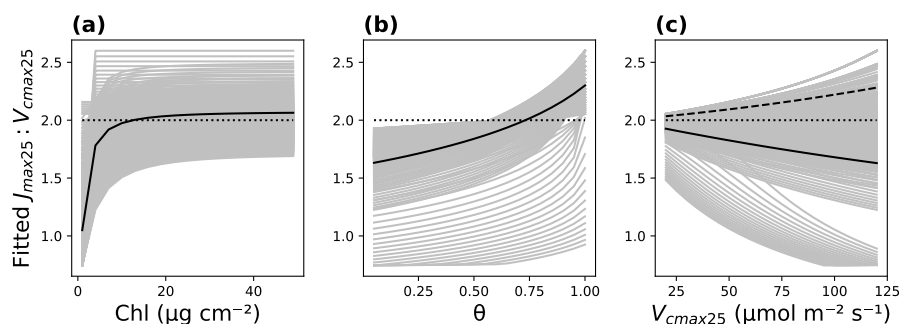


**Figure 3.** Fitted photosynthetic capacity ratio. Gray curves plot the response curves at all combinations. Solid and dashed curves plot the examples. Dotted line plot the true theoretical ratio. **(a)** Fitted ratio vs. chlorophyll content. The true  $\theta$  is 0.7, true  $V_{\max25}$  is  $80 \mu\text{mol m}^{-2} \text{s}^{-1}$ , and true  $J_{\max25}$  is  $160 \mu\text{mol m}^{-2} \text{s}^{-1}$  for the solid curve. **(b)** Fitted ratio vs.  $\theta$ . The true Chl is  $13 \mu\text{g cm}^{-2}$ , true  $V_{\max25}$  is  $80 \mu\text{mol m}^{-2} \text{s}^{-1}$ , and true  $J_{\max25}$  is  $160 \mu\text{mol m}^{-2} \text{s}^{-1}$  for the solid curve. **(c)** Fitted ratio vs.  $V_{\max25}$ . The true Chl is  $13 \mu\text{g cm}^{-2}$ , true  $\theta$  is 0.3, and true  $J_{\max25} = 2V_{\max25}$  for the solid curve. The true Chl is  $13 \mu\text{g cm}^{-2}$ , true  $\theta$  is 0.9, and true  $J_{\max25} = 2V_{\max25}$  for the dashed curve. See Table 1 for the list of symbols. The simulation are done using the Photosynthesis.jl module of the CliMA Land (Wang et al., 2021).

Our model simulation suggested that inaccurate electron quantum yield and smoothing curvature may result in substantial bias in fitted  $J_{\max25}$  (Fig. 3). This bias may impact the results related to  $J_{\max25} : V_{\max25}$  patterns (e.g., Kattge and Knorr, 2007; Walker et al., 2014). The problem of  $\alpha$  and  $\theta$  mismatch can be solved by fitting the two from measurements at different light conditions (e.g., Grassi et al., 2002); yet, the fitted values would not be ideal for a different light source. The ultimate solution to this problem would be to (i) quantify leaf biophysical properties such as pigment contents that impact leaf hyperspectral absorption features (Féret et al., 2017), (ii) compute  $f_{\text{APAR}}$  and  $f_{\text{PPAR}}$  based on the hyperspectral light source (Fig. 2), and (iii) fit  $\theta$  from measurements at different light conditions (Grassi et al., 2002).



### 3 Biased photosynthetic rate

The bias in modeled photosynthetic rates is subject to inaccurate parameterization of  $J_{\max25}$  and light source, or in other words, how different are true  $\alpha$  and  $\theta$  from those used to fit  $J_{\max25}$ . Assuming that model  $\theta$  is the same as true  $\theta$ , if true  $\alpha$  is lower than the model  $\alpha$ , the leaf actually absorbs less PAR than the model, and modeled  $J$  and thus  $A$  are overestimated. Assuming that model  $\alpha$  is the same as true  $\alpha$ , if true  $\theta$  is lower than the model  $\theta$ , modeled  $J$  and thus  $A$  are also overestimated. Depending on the model setup, there are two common scenarios where  $A$  could be biased: (1) hyperspectral leaf absorption and canopy radiative transfer schemes are used along with biased  $J_{\max25}$ , and (2) broadband leaf absorption and canopy radiative transfer schemes are used along with biased  $J_{\max25}$ . The former scenario suffers from errors in  $\theta$  and  $J_{\max25}$ , whereas the latter scenario is subject to errors in  $\alpha$ ,  $\theta$ , and  $J_{\max25}$ .

Using the second scenario as an example, when we used lower true  $\alpha$  and  $\theta$  (compared to the 0.3 and 0.7 used to estimate  $J_{\max25}$  from  $A \sim C_i$  curves), we found overestimated  $A$  (Fig. 4a). The overestimation increased with higher  $C_i$ , and increased and then decreased with higher PAR (Fig. 4a). In comparison, when we used higher true  $\alpha$  and  $\theta$ , we found underestimated  $A$  (Fig. 4b). The underestimation also increased with higher  $C_i$ , and increased and then decreased with higher PAR (Fig. 4b). Note that there is minimum bias in modeled  $A$  when PAR is high and  $C_i$  is low because  $A$  is limited by RubisCO carboxylation in this region (Fig. 4).

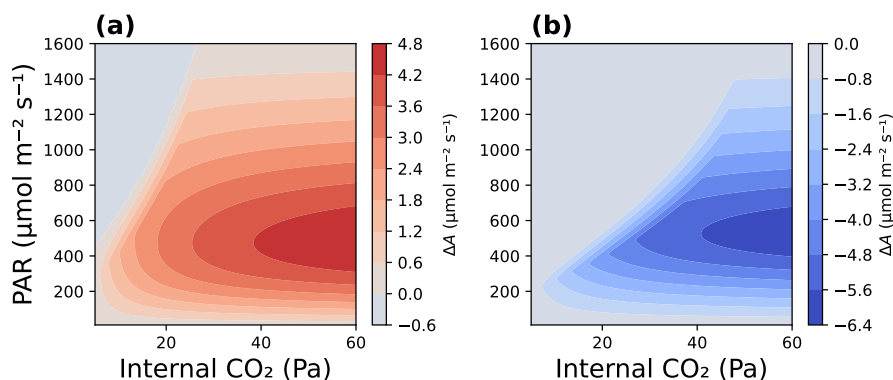


**Figure 4.** Biased photosynthetic rates (modeled value – true value) at various light and internal  $\text{CO}_2$  for C3 photosynthesis. Red color means photosynthetic rate is overestimated, and blue color means photosynthetic rate is underestimated. (a) True  $\alpha$  is 0.2, true  $\theta$  is 0.5, true  $V_{\text{cmax}25}$  is  $100 \mu\text{mol m}^{-2} \text{s}^{-1}$ , and true  $J_{\max25}$  is  $200 \mu\text{mol m}^{-2} \text{s}^{-1}$ . Model  $\alpha$  is 0.3, and model  $\theta$  is 0.7. (b) True  $\alpha$  is 0.37, true  $\theta$  is 0.9, true  $V_{\text{cmax}25}$  is  $100 \mu\text{mol m}^{-2} \text{s}^{-1}$ , and true  $J_{\max25}$  is  $200 \mu\text{mol m}^{-2} \text{s}^{-1}$ . Model  $\alpha$  is 0.3, and model  $\theta$  is 0.7. See Table 1 for the list of symbols. The simulation are done using the Photosynthesis.jl module of the CliMA Land (Wang et al., 2021).

C4 photosynthesis modeling (Collatz et al., 1992) does not require  $J_{\max25}$  or smoothing of  $J$ , and thus is biased only if  $\alpha$  is biased. When we used a lower true  $\theta = 0.2$  (compared to the default 0.3), we found overestimated  $A$  (Fig. 5a). When we used a higher true  $\alpha = 0.37$ , we found underestimated  $A$  (Fig. 5b). Like the patterns in C3 photosynthesis, the bias was minimum at high PAR and low  $C_i$ , increased with higher  $C_i$ , and increased and then decreased with higher PAR (Fig. 5).

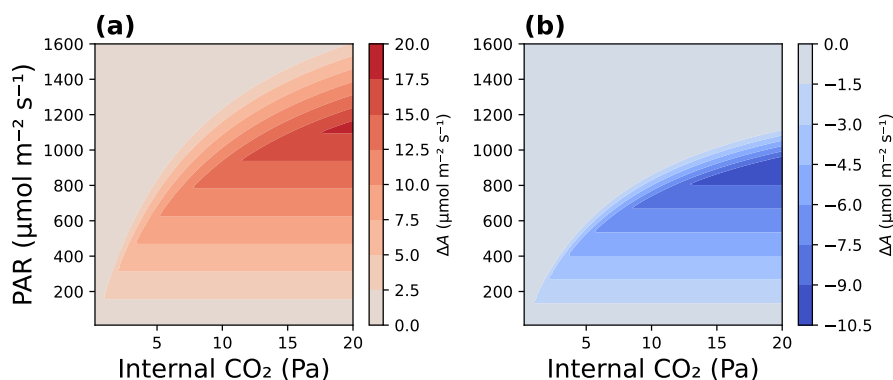


**Figure 5.** Biased photosynthetic rates (modeled value – true value) at various light and internal CO<sub>2</sub> for C4 photosynthesis. Red color means photosynthetic rate is overestimated, and blue color means photosynthetic rate is underestimated. True  $V_{c_{max25}}$  and  $V_{p_{max25}}$  are both  $80 \mu\text{mol m}^{-2} \text{s}^{-1}$ . (a) True  $\alpha$  is 0.2, whereas model  $\alpha$  is 0.3. (b) True  $\alpha$  is 0.37, whereas model  $\alpha$  is 0.3. See Table 1 for the list of symbols. The simulation are done using the Photosynthesis.jl module of the CliMA Land (Wang et al., 2021).

#### 4 Conclusions

In conclusion, inaccurate parameterization of  $\alpha$  and  $\theta$  result in bias in fitted  $J_{max25}$  and thus light-limited photosynthetic rate. Bias in  $J_{max25}$  can be positive or negative depending on the mismatch in  $\alpha$  and  $\theta$ . The absolute bias increases with higher mismatch in  $\alpha$  and  $\theta$ , and increases with higher true  $J_{max25}$  (Fig. 3). The bias in  $A$  can be overestimation or underestimation  
110 depending on the combination of  $\alpha$  and  $\theta$ ; and the absolute bias increases with higher internal CO<sub>2</sub>, and increases and then decreases with increasing radiation (Fig. 4). Given the errors caused by inaccurate model parameterization, it is recommended to move towards more complicated but more accurate and consistent modeling of light absorption in vegetation models, e.g.,  
115 (i) separation of  $\alpha$  into  $f_{APAR}$ ,  $f_{PPAR}$ ,  $f_{PSII}$ , and  $\Phi_{PSII,max}$ , and (ii) utilization of hyperspectral canopy radiative transfer and leaf light absorption, reflection, and transmission. This is especially important for leaves with low chlorophyll content, for which the assumptions of fractional PAR absorption can become highly biased, even when using artificial light.

*Author contributions.* All authors have contributed equally to this manuscript.

*Competing interests.* No competing interests



*Acknowledgements.* We gratefully acknowledge the generous support of Eric and Wendy Schmidt (by recommendation of the Schmidt Futures) and the Heising-Simons Foundation. This research has been supported by the National Aeronautics and Space Administration  
120 (NASA) Carbon Cycle Science grant 80NSSC21K1712 awarded to Christian Frankenberg.





## References

- Collatz, G. J., Ribas-Carbo, M., and Berry, J.: Coupled photosynthesis-stomatal conductance model for leaves of C4 plants, *Functional Plant Biology*, 19, 519–538, 1992.
- Evans, J. R.: Developmental constraints on photosynthesis: effects of light and nutrition, in: *Photosynthesis and the Environment*, pp. 281–304, Springer, 1996.
- Farquhar, G. D., von Caemmerer, S., and Berry, J. A.: A biochemical model of photosynthetic CO<sub>2</sub> assimilation in leaves of C<sub>3</sub> species, *Planta*, 149, 78–90, 1980.
- Féret, J.-B., Gitelson, A., Noble, S., and Jacquemoud, S.: PROSPECT-D: towards modeling leaf optical properties through a complete lifecycle, *Remote Sensing of Environment*, 193, 204–215, 2017.
- 130 Grassi, G., Meir, P., Cromer, R., Tompkins, D., and Jarvis, P.: Photosynthetic parameters in seedlings of *Eucalyptus grandis* as affected by rate of nitrogen supply, *Plant, Cell & Environment*, 25, 1677–1688, 2002.
- Harley, P. C., Loreto, F., Di Marco, G., and Sharkey, T. D.: Theoretical considerations when estimating the mesophyll conductance to CO<sub>2</sub> flux by analysis of the response of photosynthesis to CO<sub>2</sub>, *Plant Physiology*, 98, 1429–1436, 1992.
- Jacquemoud, S. and Baret, F.: PROSPECT: A model of leaf optical properties spectra, *Remote sensing of environment*, 34, 75–91, 1990.
- 135 Kattge, J. and Knorr, W.: Temperature acclimation in a biochemical model of photosynthesis: a reanalysis of data from 36 species, *Plant, cell & environment*, 30, 1176–1190, 2007.
- Lawrence, D. M., Fisher, R. A., Koven, C. D., Oleson, K. W., Swenson, S. C., Bonan, G., Collier, N., Ghimire, B., Van Kampenhout, L., Kennedy, D., Kluzek, E., Lawrence, P. J., Li, F., Li, H., Lombardozzi, D., Riley, W. J., Sacks, W. J., Shi, M., Vertenstein, M., Wieder, W. R., Xu, C., Ali, A. A., Badger, A. M., Bisht, G., van den Broeke, M., Brunke, M. A., Burns, S. P., Buzan, J., Clark, M., Craig, A., Dahlin, K., 140 Drewniak, B., Fisher, J. B., Flanner, M., Fox, A. M., Gentine, P., Hoffman, F., Keppel-Aleks, G., Knox, R., Kumar, S., Lenaerts, J., Leung, L. R., Lipscomb, W. H., Lu, Y., Pandey, A., Pelletier, J. D., Perket, J., Randerson, J. T., Ricciuto, D. M., Sanderson, B. M., Slater, A., Subin, Z. M., Tang, J., Thomas, R. Q., Val Martin, M., and Zeng, X.: The Community Land Model version 5: Description of new features, benchmarking, and impact of forcing uncertainty, *Journal of Advances in Modeling Earth Systems*, 11, 4245–4287, 2019.
- Medlyn, B. E., Dreyer, E., Ellsworth, D., Forstreuter, M., Harley, P. C., Kirschbaum, M. U. F., Le Roux, X., Montpied, P., Strassmeyer, J., 145 Walcroft, A., and Loustau, D.: Temperature response of parameters of a biochemically based model of photosynthesis. II. A review of experimental data, *Plant, Cell & Environment*, 25, 1167–1179, 2002.
- Quebbeman, J. A. and Ramirez, J. A.: Optimal allocation of leaf-level nitrogen: Implications for covariation of  $V_{\text{cmax}}$  and  $J_{\text{max}}$  and photosynthetic downregulation, *Journal of Geophysical Research: Biogeosciences*, 121, 2464–2475, 2016.
- Smith, E. L.: The influence of light and carbon dioxide on photosynthesis, *The Journal of general physiology*, 20, 807–830, 1937.
- 150 Sperry, J. S., Venturas, M. D., Anderegg, W. R. L., Mencuccini, M., Mackay, D. S., Wang, Y., and Love, D. M.: Predicting stomatal responses to the environment from the optimization of photosynthetic gain and hydraulic cost, *Plant, Cell & Environment*, 40, 816–830, 2017.
- van der Tol, C., Berry, J., Campbell, P., and Rascher, U.: Models of fluorescence and photosynthesis for interpreting measurements of solar-induced chlorophyll fluorescence, *Journal of Geophysical Research: Biogeosciences*, 119, 2312–2327, 2014.
- von Caemmerer, S.: Updating the steady-state model of C4 photosynthesis, *Journal of Experimental Botany*, 72, 6003–6017, 2021.
- 155 Walker, A. P., Beckerman, A. P., Gu, L., Kattge, J., Cernusak, L. A., Domingues, T. F., Scales, J. C., Wohlfahrt, G., Wullschlegel, S. D., and Woodward, F. I.: The relationship of leaf photosynthetic traits— $V_{\text{cmax}}$  and  $J_{\text{max}}$ —to leaf nitrogen, leaf phosphorus, and specific leaf area: A meta-analysis and modeling study, *Ecology and Evolution*, 4, 3218–3235, 2014.



- 160 Wang, Y., Köhler, P., He, L., Doughty, R., Braghieri, R. K., Wood, J. D., and Frankenberg, C.: Testing stomatal models at the stand level in deciduous angiosperm and evergreen gymnosperm forests using CliMA Land (v0.1), *Geoscientific Model Development*, 14, 6741–6763, 2021.
- Wullschleger, S. D.: Biochemical limitations to carbon assimilation in C3 plants—a retrospective analysis of the A/Ci curves from 109 species, *Journal of experimental botany*, 44, 907–920, 1993.